Progress In Electromagnetics Research, PIER 101, 277–290, 2010

EFFECT OF ATMOSPHERIC PROPAGATION IN RCS PREDICTIONS

A. Alexopoulos

Electronic Warfare and Radar Division
Defence Science and Technology Organisation (DSTO)
P. O. Box 1500, 180L Edinburgh 5111, Australia

Abstract—We consider how an electromagnetic field propagating to a target alters the radar cross section of the target relative to an observer. We derive the optimum high-frequency path for the fields using the calculus of variations and by using a realistic refractive index profile for the atmosphere obtain closed form solutions. It is found that the predicted nulls and peaks in the radar cross section of a scattering object relative to an observer are shifted from those normally expected from just the isolated object. Hence, for predictive purposes at least, radar cross section results need to incorporate the effects of atmospheric propagation.

1. INTRODUCTION

The radar cross section (RCS) σ [1–3] of many objects is routinely determined by experimental measurements inside laboratories or anechoic chambers. These measurements give the σ profile for the isolated object alone without any regard as to what effect the surrounding medium has on the results. One objective is to understand the RCS signature of the object so that one can try to manipulate it according to specific needs. In order to make a more informed theoretical prediction of the RCS of flying platforms in particular, the effects due to the medium they operate in needs to be taken into account. For instance, the perceived RCS of an aircraft will differ from its static profile measured on the ground due to the fact that the atmospheric refractive index changes important parameters. If we are interested in devising means of reducing the RCS of an aircraft, we need to know what the perceived electromagnetic signature is for a radar system on the earth's surface relative to the position

Corresponding author: A. Alexopoulos (Aris.Alexopoulos@dsto.defence.gov.au).

of the aircraft at a certain height. This allows one to understand variations in the RCS for operational advantages. The purpose of this paper is to look at some of these issues and see if in fact there is any important variation that needs to be accounted for in general prediction studies. The realistic scenario considered here is solved in closed form and avoids numerical computations. It is shown that the RCS is dependent on the radar (observer) location and this dependence comes about because of the refractive index profile of the atmosphere. The non-linear trajectories of the fields to the scattering target are determined in the high-frequency limit using the calculus of variations [4–7] in order to find the optimal path. This approach is analogous to Fermat's principle of least time. The resulting equations must be evaluated numerically for most cases, however we show that it is possible to solve the differential equation analytically. From these results we discuss other scattering parameters of interest. The method presented can be used to model and predict more complicated scenarios involving ducts, multi-path and bi-static propagation effects as well as improving the results in time difference of arrival (TOA) calculations of radar signals. Overall, the results are important for the correct characterisation of target heights and distances as well as general phase effects in signal propagation. In most problems concerning scattering, the effect that the propagating medium has on the scattering object for electromagnetic waves traveling from a source at a distance is neglected due to the complexity involved in determining the actual trajectories of the fields. In the case of the latter, ray tracing methods are used for the determination of such paths but these involve numerical and computationally intensive algorithms [8–12]. On the other hand the same applies for calculations involving the solution of Maxwell's equations. Analytic methods using asymptotic techniques and ray transfer matrix analysis have been presented [13] but these approaches are mathematically too difficult to implement for general atmospheric profiles. In what follows we will show that, via the use of the calculus of variations, it is possible that a simple equation can be derived for application in atmospheric propagation and scattering problems concurrently without the need to perform any overly complex computations for the propagation and scattering independently. Thus for most atmospheric profiles, the solutions can be obtained analytically which can then be used in scattering calculations. In cases where the solutions cannot be solved analytically, a simple numerical integration can be used instead.

2. EXTREMUM OF THE ELECTROMAGNETIC FIELD PATHS

We consider the case where an electromagnetic field propagates to a scattering object in a non-homogeneous medium such as the atmosphere. It would appear that there are many possible paths that can be considered. However in reality, for a given refractive index, there is only one optimal path considered by the fields and to determine it requires calculating such a trajectory as an extremum over all the possible paths that can be taken. Hence, in order to determine this path we start with the optimal distance traversed by the fields and define it as s:

$$ds^2 = \sum_{i=1}^{2}\sum_{j=1}^{2} r_{ij}dx_i dx_j = r_{11}(dx)^2 + (r_{12}+r_{21})dxdy + r_{22}(dy)^2 \quad (1)$$

where $dx_1 = dx$ and $dx_2 = dy$. We define r_{ij} to be a square two-dimensional refractive index matrix that dictates how the fields propagate in the medium (atmosphere). If the fields are propagating in the atmosphere then the paths are modified from the linear form by the refractive index. Typically, there are no variations in the refractive index with range x so we set $x = x_0$ to be a constant and since the actual variation is with height we assume that the refractive index changes with y thus we have a refractive index with arguments: $n(x_0, y(x))$. This also implies that since there is variation with height the fields are affected by the elevation θ while the azimuth ϕ is constant. Note that, since the azimuth angle is not important in this analysis, the symbol ϕ will from this point on, be used as shown in Fig. 1. From these assumptions, we define the refractive index matrix as,

$$r_{ij} = \begin{pmatrix} n^2(x_0, y(x)) & 0 \\ 0 & n^2(x_0, y(x)) \end{pmatrix} \quad (2)$$

where in what follows we will omit x_0 for brevity reasons. We also note that the off-diagonal terms of the matrix are zero because there is no 'coupling' or variation in the refractive index with range *and* height, but only in height. Equation (1) now becomes

$$s = \int \sqrt{r_{11} + r_{22}\left(\frac{dy}{dx}\right)^2}\, dx \quad (3)$$

Substituting the components of the refractive index matrix (2) into (3) we have

$$s = \int n(y(x))\sqrt{1 + \left(\frac{dy}{dx}\right)^2}\, dx \quad (4)$$

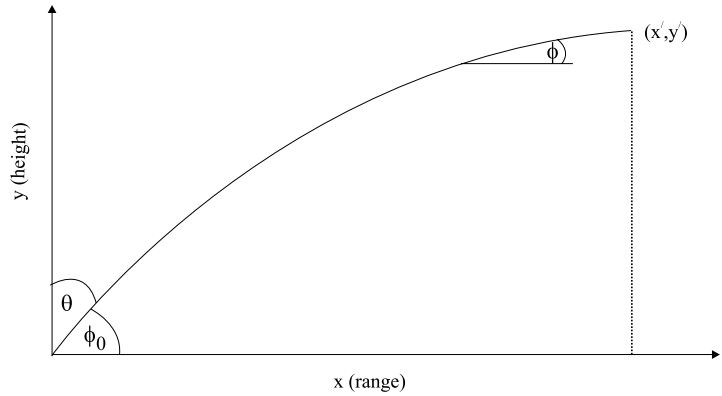

Figure 1. Shown is the curved path the fields actually propagate along compared to the normal method of assuming linear trajectories. The curved path is due to the refractive index of the atmosphere. As a result, the angle of radiation from the origin ϕ_0 in not the same as the incident angle at the scattering object ϕ — see also Fig. 2. The angle θ is the elevation but we are more interested in the angles ϕ_0 and ϕ in the analysis.

In order to find the optimal path that the field propagates along we have to solve for the extremum of (4). Let

$$L = n(y(x))\sqrt{1 + \left(\frac{dy}{dx}\right)^2} \tag{5}$$

From the calculus of variations we make use of the well known Euler-Lagrange equation in order to derive a differential equation that gives the extremum for the path taken by the fields or put another way, we derive the trajectory of least time, also known as Fermat's principle. Thus we have,

$$\frac{\partial L}{\partial y} - \frac{d}{dx}\left(\frac{\partial L}{\partial (dy/dx)}\right) = 0 \tag{6}$$

Using (5) we can evaluate the first term in (6) which becomes

$$\frac{\partial L}{\partial y} = \frac{\partial n(y(x))}{\partial y}\sqrt{1 + \left(\frac{dy}{dx}\right)^2} \tag{7}$$

The second remaining term in the Euler-Lagrange equation can now

be determined, so once again by the use of (5) we have

$$\frac{d}{dx}\left(\frac{\partial L}{\partial(dy/dx)}\right) = \left[1+\left(\frac{dy}{dx}\right)^2\right]^{-3/2}\left\{\frac{\partial n(y(x))}{\partial y}\left[\left(\frac{dy}{dx}\right)^2+\left(\frac{dy}{dx}\right)^4\right]+n(y(x))\frac{d^2y}{dx^2}\right\} \quad (8)$$

Combining (7) and (8) and simplifying gives the result

$$\frac{d^2y}{dx^2} - \frac{1}{n(y(x))}\frac{\partial n(y(x))}{\partial y}\left[1+\left(\frac{dy}{dx}\right)^2\right] = 0 \quad (9)$$

The solution of (9) gives the so called path of least action of the fields propagating in the atmosphere with refractive index $n(y(x))$ and as it stands is a very complicated expression to solve, especially in closed-form. Fortunately (9) can be factored to the form

$$\frac{d}{dx}\left[\frac{1}{n(y(x))}\sqrt{1+\left(\frac{dy}{dx}\right)^2}\right] = 0 \quad (10)$$

Integrating (10) we have

$$\int \frac{d}{dx}\left[\frac{1}{n(y(x))}\sqrt{1+\left(\frac{dy}{dx}\right)^2}\right]dx = \alpha \quad (11)$$

where we notice that the left-hand side is its own anti-derivative while α is the integration constant. Re-arranging (11) we finally have

$$\frac{dy}{dx} = \sqrt{\alpha^2 n^2(y(x)) - 1} \quad (12)$$

The solution of (12) gives the optimum variation of the fields with height y as a function of the range x for a given refractive index profile. Equation (12) has solution as given by

$$y(x) = y_0 + \int_{x_0}^{x} dx\sqrt{\alpha^2 n^2(y(x)) - 1} \quad (13)$$

From this expression we can now obtain the actual optimal (extremum) distance that the fields travel which becomes

$$s = \alpha \int_{x_0}^{x} n^2(y(x))dx \quad (14)$$

Equation (14) gives the actual distance that the electromagnetic field travels to a target compared to the direct line of sight linear

distance assumed in many situations. Equation (14) has an integrand containing an arbitrary refractive index profile written as a function of the optimised field path. What this means is that, depending on the refractive index profile considered, the actual distance to a target will vary from the assumed direct line of sight (linear) distance used in most situations especially in elevated or surface ducts with targets over the horizon. It is also worth noting that a scattering target containing a cavity for example, adds to the overall distance the target is assumed to be at because the fields bounce around inside the cavity for a distance that varies with initial scattering incident angle ϕ. The more complicated the cavity, the more time spent by the fields inside, hence the target distance varies accordingly. We can see this effect even for a simple circular cavity of length l which would modify (14) to

$$s = \frac{2l}{\cos(\phi)} + 2\alpha \int_{x_0}^{x} n^2(y(x))dx \tag{15}$$

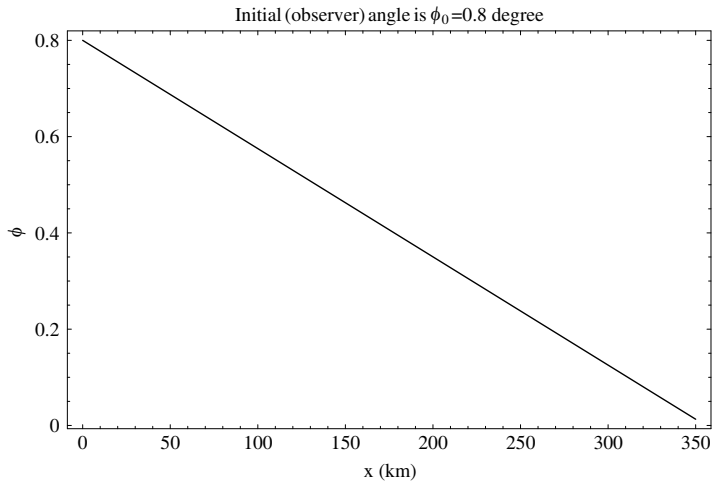

Figure 2. The incident scattering angle ϕ changes (with respect to the horizon) for a target at any arbitrary point along the distance s that the fields propagate on. As a consequence the angle of incidence ϕ at the scattering object is not the same as the initial radiated angle ϕ_0. Here we see the predicted angular variation with range x for the parameters considered in the SBF model of Section 3. In more general problems, this variation is not necessarily linear as shown here and can change dramatically in a non-linear way.

where the factor '2' accounts for the two-way distance, i.e., observer to target and back. This effect is highly dependent on the structure of the cavity but also more generally on the incident angle ϕ as shown for the parameters considered here in Fig. 2. Fig. 3 shows the additional distance that is traveled by the fields in such a cavity (this is the first term in (15)) of length $l = 4\,\mathrm{m}$. As the cavity aspect angle changes around the incident scattering angle ϕ at the cavity entrance, the target distance as given by (15) is increased even more by the fact that fields have to travel an additional distance inside the cavity and all this must be related to the observer at angle ϕ_0. The results discussed so far indicate that other issues need to be accounted for such as phase differences due to perturbations in distances and time (time of arrival TOA) and so on. In any event all of these effects rely on the most important parameter of all, i.e., the arbitrary refractive index profile $n(y(x))$ which means that (13) has to be solved numerically for any practical study of such effects. In the next section however, we shall investigate a realistic refractive index model which is extremely accurate, especially for low altitudes, and will allow us to obtain solutions in closed form. This is the so called Schelling, Burrows and Ferrell refractive index model (SBF) [14–16].

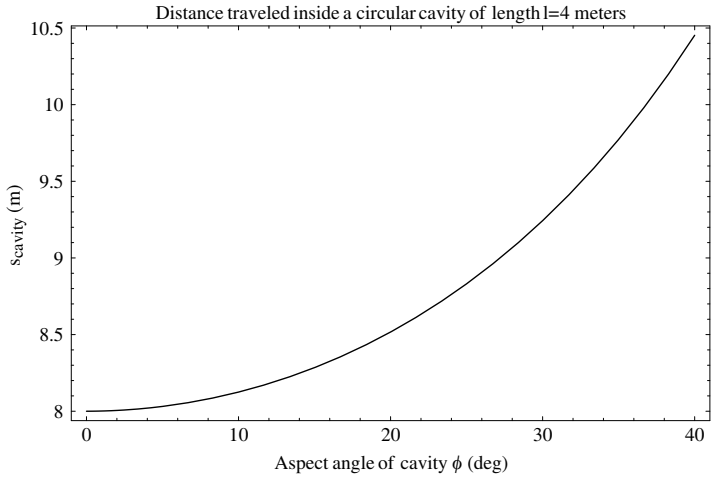

Figure 3. As the cavity rotates around the incident scattering angle and in relation to an observer with angle ϕ_0 on the ground, the distance traveled inside the cavity by the fields changes which directly alters further the correct distance to the target as given by (15). Here we take the observer angle as $\phi_0 = 0.8$ degrees and the cavity structure is at $x = 350\,\mathrm{kms}$. A more complex and/or longer cavity will have a much greater effect than the case considered here.

3. OPTIMAL SOLUTIONS BASED ON THE SBF MODEL

The SBF model for the refractive index of the atmosphere has been shown to be quite accurate for heights of up to 3 km but is less accurate as the height increases above that [14–16]. However, given its accuracy for the heights concerned and the fact that it has linear form, it will be used to obtain analytic solutions which will allow the study of how the atmosphere affects propagation to a target and therefore, how it changes the RCS characteristics of that target. Consequently, if the latter is true for smaller heights, then these effects will be greater for increased heights or in cases where other atmospheric issues are important, such as ducts, multi-path and bi-static propagation respectively. In the SBF approach, the refractive index is defined to be:

$$n(y(x)) = n_0\,(1 - \beta y(x)) \tag{16}$$

where β is a constant and n_0 is the refractive index at the radiating source of the electromagnetic waves, e.g., close to the earth so that $n_0 \approx 1$. Returning to our previous derivation for the optimum path of the fields we consider the form,

$$\frac{dy}{dx} = \sqrt{\alpha^2 n^2(y(x)) - 1} \tag{17}$$

For fields radiating from say the origin $(x, y) = (0, 0)$ at an angle ϕ_0 (as measured from the range axis, i.e., x), then $y'(0) = \tan(\phi_0)$ at $x = 0$ while $y(0) = 0$. This allows us to work out the integration constant

$$\alpha = \frac{1}{n_0 \cos(\phi_0)} \tag{18}$$

From this and re-arranging (17) we have:

$$dx = \frac{\cos(\phi_0)dy}{\sqrt{(1 - \beta y)^2 - \cos^2(\phi_0)}} \tag{19}$$

From Fig. 1, we notice that the complementary angle θ is related to ϕ by $\theta = \pi/2 - \phi$, hence we can make use of the trigonometric identity,

$$1 - \beta y = \cos(\phi_0)\sec(\theta) \tag{20}$$

with $\theta = \phi_0$ at $y = 0$. Thus,

$$dy = -\frac{\cos(\phi_0)}{\beta}\sec(\theta)\tan(\theta)d\theta \tag{21}$$

and

$$\sqrt{(1 - \beta y)^2 - \cos^2(\phi_0)} = \cos(\phi_0)\tan(\theta) \tag{22}$$

Then (17) now becomes

$$dx = -\frac{\cos(\phi_0)}{\beta}\sec(\theta)d\theta \tag{23}$$

and solving this equation for $x = 0$ when $\theta = \phi_0$ we have,

$$x = -\frac{\cos(\phi_0)}{\beta}\log_e\left(\frac{\sec(\theta)+\tan(\theta)}{\sec(\phi_0)+\tan(\phi_0)}\right) \tag{24}$$

Let us define,

$$\gamma = \frac{\beta x}{\cos(\phi_0)} - \log_e\left(\sec(\phi_0)+\tan(\phi_0)\right) \tag{25}$$

then (24) becomes:

$$\sec(\theta) + \sqrt{\sec^2(\theta)-1} = e^{-\gamma} \tag{26}$$

which can now be solved for $\sec(\theta)$ to give,

$$\sec(\theta) \equiv \cosh(\gamma) = \cosh\left(\frac{\beta x}{\cos(\phi_0)} - \log_e\left(\sec(\phi_0)+\tan(\phi_0)\right)\right) \tag{27}$$

Finally, using (20) and these results we obtain the optimised path for the fields traveling in the atmosphere with refractive index as given by the SBF model as being:

$$y(x) = \frac{1}{\beta} - \frac{\cos(\phi_0)}{\beta}\cosh\left(\frac{\beta x}{\cos(\phi_0)} - \log_e\left(\sec(\phi_0)+\tan(\phi_0)\right)\right) \tag{28}$$

If the refractive index was constant for all height values then we would expect that the paths taken by the fields would be straight lines and in fact by assuming that $n(y) = n_0$ and using (17) we find exactly this as we obtain the solution $y(x) = \tan(\phi_0)x$, with initial conditions given at $(x, y) = (0, 0)$. Finally, from (28) we can obtain the maximum height $y = y'$ of the field trajectories with corresponding range $x = x'$ before they start to curve downwards-see Fig. 1:

$$y'(x) = y'(\beta) = \frac{1-\cos(\phi_0)}{\beta} \tag{29}$$

and which occurs at the range:

$$x' = x'(\beta) = \frac{\cos(\phi_0)}{\beta}\log_e\left(\sec(\phi_0)+\tan(\phi_0)\right) \tag{30}$$

From Fig. 1, the angle ϕ that the trajectory of the field makes with a target at any arbitrary point is given by

$$\phi = \tan^{-1}\left(\sinh\left(\log_e(\sec(\phi_0)+\tan(\phi_0)) - x\beta\sec(\phi_0)\right)\right) \tag{31}$$

In all of these expressions, the constant β determines the curvature of the trajectories in the atmosphere. In the SBF model, the value we choose is $\beta = (4r_0)^{-1}$ [15], where r_0 is the radius of the earth. In the next section we will make use of these results to see if RCS predictions are affected by the refractive index at all and whether correct modeling of the field trajectories are necessary for the correct prediction of general RCS.

4. RCS PREDICTIONS

The dimensions of the scatterers we will consider are much greater than the size of the wavelength so in order to obtain the RCS σ we will make use of the physical optics (PO) limit [17–21]. We consider two types of targets that are situated at a given height y and range x and determine the RCS 'observed' by a radar at a given angle. Generally it is assumed that the angle of the observer and the scattering angle at the target are the same and this would be true if we considered an atmosphere with no refractive index. However given that the atmosphere has varying refractive index profiles, the paths of electromagnetic fields in the high-frequency approximation follow the optimised path as determined in the previous section. Since the angle of the observer and the scattering angle are different, we can see what effect this has on the RCS of a flat plate and a rectangular cavity as measured by an observer on the ground.

It should be emphasised that because of the reciprocity in the results we can assume that instead of having the radar (observer) at ground level and the plate and cavity at a given height (e.g., aircraft hull or engine intake), we can also assume that the results hold for a radar at a height y scanning a flat plate or rectangular target at ground level (e.g., vehicle or missile pods). For a rectangular flat plate the RCS is given by [22, 23]:

$$\sigma = \frac{4\pi a^2 b^2}{\lambda^2} \cos^2(\phi) \left[\frac{\sin(ka \sin(\phi))}{ka \sin(\phi)} \right]^2 \tag{32}$$

where the wave number is $k = 2\pi/\lambda$ and ϕ is the incident angle to the plate with respect to the observer. We will assume that the plate is rotated around ϕ while the observer is fixed, while we note that this could also be the other way around. Here we take a and b as being the physical side dimensions of the flat plate and λ is the wavelength. The RCS for a rectangular cavity of side lengths a, b and depth c can be

obtained from [22, 23]:

$$\sigma = \frac{4\pi c^2}{\lambda^2}\left|a\cos(\phi)\mathrm{sinc}(ka\sin(\phi))e^{ikb\cos(\phi)}\right. \\ \left. +b\sin(\phi)\mathrm{sinc}(kb\cos(\phi))e^{ika\sin(\phi)}\right|^2 \tag{33}$$

The theoretical RCS values obtained from (32) and (33) neglect polarisation since in the PO approach the theory does not include polarisation dependence. It is also worth noting that for small scattering angles in particular (32) and (33) are in excellent agreement with experimental results and GTD/UTD calculations [22]. Figs. 4 and 5 respectively show the RCS predicted for scattering from a plate and rectangular cavity structure. The results show that the SBF atmospheric model predicts changes in the radar cross section of targets at a given height and range, even when the initial radiating angle of the electromagnetic waves is small. Specifically, the assumed maxima or minima in the scattering profiles are shifted due to the fact that the scattering angle at the target is not the same as the initial

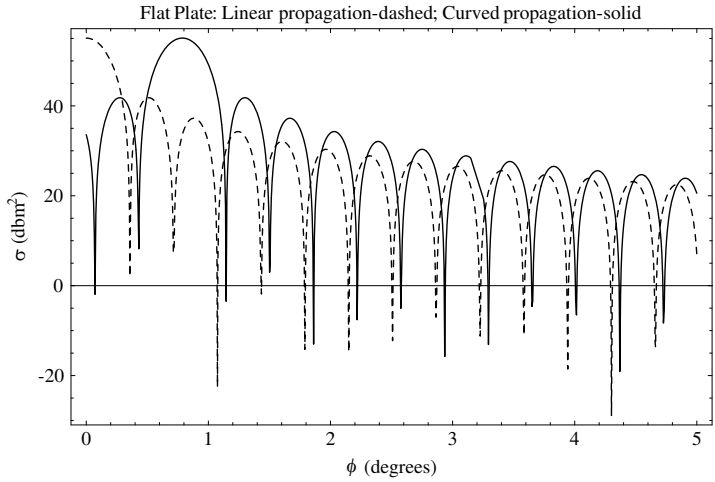

Figure 4. Physical optics scattering limit for a flat plate of side dimensions $a = 2\,\mathrm{m}$ and $b = 2\,\mathrm{m}$ respectively. The frequency is at $f = 12\,\mathrm{GHz}$ and the observer angle is at $\phi_0 = 0.8\,\mathrm{deg}$. As the plate is rotated around ϕ the expected RCS profile is changed compared to the normal direct linear path (dashed) due to the angle of observer and scattering angle being different as a consequence of the refractive index of the propagating medium. Position of scatterer is at $x = 350\,\mathrm{km}$.

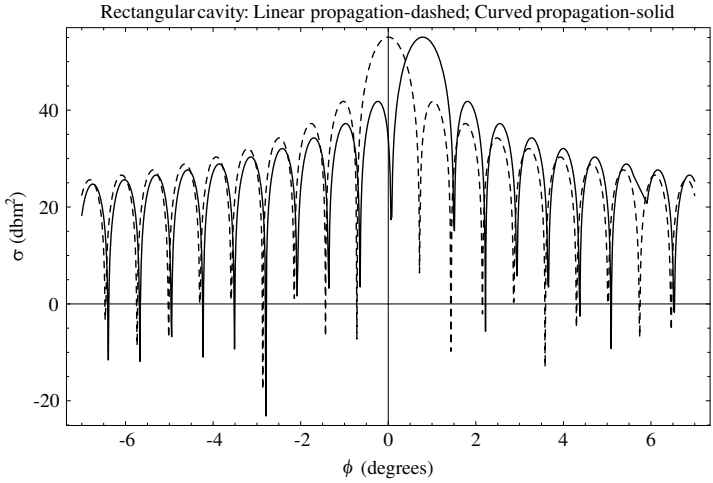

Figure 5. RCS σ in the physical optics limit for a rectangular cavity with side dimensions $a = 1\,\mathrm{m}$, $b = 1\,\mathrm{m}$ and depth of $c = 4\,\mathrm{m}$ at a frequency of $f = 12\,\mathrm{GHz}$. The dashed profile is the RCS of the cavity for a linear atmosphere which corresponds to the same angles for both observer on the ground and scattering angle at cavity. The atmospheric refractive index alters the RCS as shown by the solid profile since the observer angle (here taken as $\phi_0 = 0.8\,\mathrm{deg.}$) is *not* the same as the scattering angle at the cavity. Position of scatterer is at $x = 350\,\mathrm{km}$.

radiating angle. Hence, a target can practically minimize it's RCS characteristics and falsify its actual signature via knowledge of the effect that the atmospheric profile has on the scattering parameters. Modeling such scattering under realistic scenarios incorporating the effects of the propagating medium is paramount for general RCS reduction or signature transformation purposes. For example in the understanding of how one might reduce the RCS of an air platform as observed by a sensor on the ground requires the inclusion of an analysis such as the one presented in this paper. Evidently these effects are even more pronounced for situations pertaining to RCS predictions due to ducts and multipath scattering. At the same time, phase effects, time variations, true target heights and distances can be predicted by such an analysis.

5. CONCLUSION

Analysis shows that for predictive RCS we require a proper understanding of the effects of atmospheric propagation. Using the Euler-Lagrange equation we have derived a differential equation that can be solved for general cases of refractive index. These results enable us to derive scattering parameters which show that there is variation of the RCS for a plane and cavity struture respectively at a given height and range due to atmospheric refraction. Closed-form solutions were obtained for the Schelling-Burrows-Ferrel atmospheric model.

REFERENCES

1. Ruck, G. T., D. E. Barrick, W. D. Stuart, and C. K. Krichbaum, *Radar Cross Section Handbook*, Vol. 1 and 2, Plenum Press, 1970.
2. Knott, E. F., J. F. Shaeffer, and M. T. Tuley, *Radar Cross Section*, Artech House, Norwood, 1985.
3. Stratton, J. A., *Electromagnetic Theory*, McGraw-Hill, New York and London, 1941.
4. Gelfand, I. M. and S. V. Fomin, (Translated and edited by Silverman, R. A.), *Calculus of Variations*, Dover Edition, 2000.
5. Ewing, G. M., *Calculus of Variations with Applications*, Dover, New York, 1985.
6. Bolza, O., *Lectures on the Calculus of Variations*, Dover, New York, 1961.
7. Forsyth, A. R., *Calculus of Variations*, Dover, New York, 1960.
8. Ng, K. H., E. K. Tameh, and A. R. Nix, "A new hybrid geometrical optics and radiance based scattering model for ray tracing applications," *IEEE Int. Conf. Comm.*, 2168–2172, 2005.
9. Rawlinson, N., J. Hauser, and M. Sambridge, "Seismic ray tracing and wavefront tracking in laterally heterogeneous media," *Advan. in Geophys.*, Vol. 49, 203–267, 2007.
10. Cocheril, Y. and R. Vauzelle, "A new ray-tracing based wave propagation model including rough surfaces scattering," *Progress In Electromagnetics Research*, PIER 75, 357–381, 2007.
11. Maystre, D., "Electromagnetic scattering by a set of objects: An integral method based on scattering operator," *Progress In Electromagnetics Research*, PIER 57, 55–84, 2006.
12. Deschamps, G. A., "Ray techniques in electromagnetics," *Proc. IEEE*, Vol. 60, No. 9, 1022–1035, 1972.
13. Alexopoulos, A., "Resonance effects in electromagnetic propaga-

tion using a modified J. W. K. B. approach," *IEEE Proc. Rad. 06*, 288–295, 2006.

14. Schelling, J. C., C. R. Burrows, and E. B. Ferrell, "Ultra-short wave propagation," *Proc. of IRE*, Vol. 21, No. 5, 427–463, 1933.
15. Blake, L. V., *Radar-performance and Analysis*, Artech-House, 1986.
16. Bean, B. R. and G. D. Thayer, "Models of the atmospheric radio refractive index," *Proc. of IRE*, Vol. 47, No. 5, 740–755, 1959.
17. Alexopoulos, A., "Asymptotic solutions to multidimensional rapidly-oscillating integrals," *Electron. Lett.*, Vol. 44, No. 10, 610–612, 2008.
18. Akhmanov, A. and S. Y. Nikita, *Physical Optics*, Oxford University Press, 1997.
19. Asvestos, J. S., "The physical optics method in electromagnetic scattering," *J. Math. Phys.*, Vol. 21, No. 2, 290–299, 1980.
20. Umul, Y. Z., "Modified theory of physical optics," *Optics Express*, Vol. 12, No. 80, 4959–4972, 2004.
21. Gordon, W. B., "High-frequency approximations to the physical optics scattering integral," *IEEE Trans. Antennas Propag.*, Vol. 42, No. 3, 427–432, 1994.
22. Anderson, W. C., "The radar cross section of perfectly-conducting rectangular flat plates and rectangular cylinders — A comparison of physical optics, GTD and UTD solutions," DSTO Report ERL-0344-TR, 1985.
23. Balanis, C. A., *Advanced Engineering Electromagnetics*, Wiley, 1989.